IAC-19,C2,2,11,x54812

TriTruss: A New and Novel Structural Concept Enabling Modular Space Telescopes and Space Platforms

William Doggett[1*], John Dorsey[1], Tom Jones[1], Martin Mikulas[2], John Teter[3], David Paddock[3]

[1]Structural Mechanics and Concept Branch, NASA Langley Research Center, Hampton VA
[2]National Institute of Aerospace, Hampton VA
[3]Mechanical Systems Branch, NASA Langley Research Center, Hampton VA
* Corresponding Author

Abstract

Modular structures that can be assembled on-orbit will be the backbone for all future persistent missions, including in-space assembled telescopes and platforms for science and communications. The TriTruss is a new and innovative structural module that has been conceived by researchers at the NASA Langley Research Center for platform and telescope applications. Some of the innovative features of the TriTruss include: very compact packaging for launch, the possibility of staged packaging, simple robotic deployment, ease of embedding payload components, an innovative structural connector that has linear structural performance, ease of module-to-module robotic assembly, design versatility, and ease of customizing its design for specific applications. This paper will introduce the TriTruss concept and describe how it can serve as the foundation for many different mission applications, in particular, a 20-meter diameter large space telescope and a beam-type platform that can host a variety of payloads and instruments. The geometry of the TriTruss will be described and the various truss design variables (such as truss depth, member diameter, material modulus, etc.) and each of their impacts on the truss performance will be illustrated. The TriTruss can be mapped to a variety of structural forms, such as beams, two-dimensional platforms and filled curved apertures (for antennas and telescopes), and examples will be illustrated. The TriTruss lends itself to a large variety of packaging schemes; the structural concepts associated with packaging and deployment will be described, as well as the means for robotically deploying TriTruss modules and locking them into their final configuration. TriTruss module-to-TriTruss module robotic assembly operations will also be described. Equations will be presented to structurally size TriTruss modules, such that when assembled into the final persistent platform, the platform achieves a desired level of global structural performance. A status of the TriTruss development will also be presented. This material will cover design and fabrication of TriTruss hardware for platform and telescope applications as well as structural testing of that hardware (the struts, connectors and platforms). Robotic assembly of TriTruss modules is also being performed, and the results of those tests will be summarized.

Keywords: In-Space Assembly (ISA), Space Telescope, TriTruss, Modular Assembly.

Nomenclature

a - Surface member length as defined in Fig. 3f
Ap - Area of a single hex panel as given in equation 3
As - Cross sectional area of surface members
Cf - Frequency equation constant = 3.345 for free-free circular plate (see equation 6)
$DPlate$ - Effective plate bending stiffness of reflector truss (see equation 4)
$Deff$ - Effective diameter of reflector consisting of Nmodules (see equation 2)
$Dmax$ - Maximum diameter of multi-ring hexagonal panel reflector (see equation 7)
$Dstrut$ - Diameter of strut calculated from As and assumed strut thickness, t
Ec - Modulus of surface members
f - First free-free bending frequency of reflector including panel and truss mass
H - Module height or truss depth following assembly of multiple TriTruss modules as defined in Fig. 3f
JF - Joint factor to account for joint mass used in Appendix A

$Nmodules$ - Number of TriTruss modules, Fig. 3. = $3r^2 + 3r + 1$
mp - Mass per unit area of hexagonal surface panels used in Appendix A
m - Total mass per unit area of panels and trusses used in Appendix A
$MTriTruss$ - Mass of TriTruss consisting of Nmodules
r - Number of module rings, as defined by the different color zones in Fig. 6a (3 rings are shown)
t - Assumed strut thickness used in Appendix A
α - Ratio of truss depth, H, to surface member length, a, ($\alpha = H/a$)
β - Ratio of cross-sectional area of all the core members to the cross-sectional area of surface members
ρ - strut density used in Appendix A

Acronyms/Abbreviations

ISA - In-Space Assembly
PA - Persistent Asset: any near zero-gravity or planetary surface system that benefits from multiple visits

1. Introduction and Background

Space operations are on the cusp of a revolutionary new operational paradigm that leverages modular systems and repeated robotic visits to "Persistent Assets" enabling asset maintenance, repair, and enhancement. A "Persistent Asset" (PA) is defined here as any near zero-gravity (zero-g) or planetary surface system that benefits from multiple visits. These visits can be used for assembly, servicing, repairs, reconfiguration, and upgrades.[1-5] Several companies are developing vehicles and robotic assets to support these operations.[5, 8] Two examples of PAs are depicted in Fig. 1, a large orbiting platform such as a power beaming system or space tug on the left and a large space telescope on the right. The term "Persistent Asset" encompasses not only zero-g systems, such as telecommunication platforms [9], Earth observing science platforms, Department of Defense persistent platforms, and scientific telescope systems [7], but also planetary surface systems.[10,12] The term "Persistent" is used to emphasize that the asset has a long lifespan. Although In-Space Assembly (ISA) has been predicted for decades (Hedgepath, Mikulas) [13] as a means of achieving PAs, it is only recently that the commercial need for methods to reliably modify on-orbit spacecraft capabilities has become critical. This has been enabled by the emergence of a new lower cost launch infrastructure, the rapid advancement of electronic system technology, and the increased competition from alternate approaches, such as shorter life low-Earth-orbit constellations. This need makes it imperative to upgrade systems more frequently than the 15+ year lifespan of existing systems. In addition, to remain competitive, satellite operators need approaches to rapidly respond to changes in customer requirements. These needs, coupled with the advent of low-cost launch providers [14] and proven reliable operation of space manipulation systems with high degrees of autonomy [15-19] has created a unique environment for the adoption of a PA operational paradigm.

The Persistent Asset paradigm, introduced, defined and extensively described in [20], includes the following attributes: 1) provides rapid emplacement of capabilities followed by planned upgrades and enhancement; 2) benefits from multiple visits; 3) can be anywhere in space (near zero-g or planetary surface); 4) incorporates modular systems and connectors; 5) enables modules to be integrated and tested before launch; 6) modules can be assembled, serviced, repaired, exchanged, etc.; 7) emphasis on robotic (as opposed to crew) interactions; 8) modular components are launch-vehicle agnostic; 9) space operations make use of a standard toolbox of technologies, capabilities, and infrastructure tools; and 10) modules can be reused for multiple missions.

From the preceding attributes, successfully architecting and designing modular systems (such as structures) and their associated modular connectors is key to realizing the next generation of efficient space systems. Modular structures that can be assembled on-orbit will be the backbone for all future persistent missions, including in-space assembled telescopes and platforms for science and communications (Fig. 1). The TriTruss is a new and innovative structural module that has been conceived by researchers at the NASA Langley Research Center for near zero-g platform and telescope applications. The TriTruss structural concept has been specifically designed to embrace the design for persistence paradigm. Some of the innovative features of the TriTruss include: very compact packaging for launch, the possibility of staged packaging, simple robotic deployment, ease of embedding payload components, an innovative structural connector that has linear structural performance, ease of module-to-module robotic assembly, design versatility, and ease of customizing its design for specific applications.

a) Generic Persistent Platform   b) Large Space Telescope
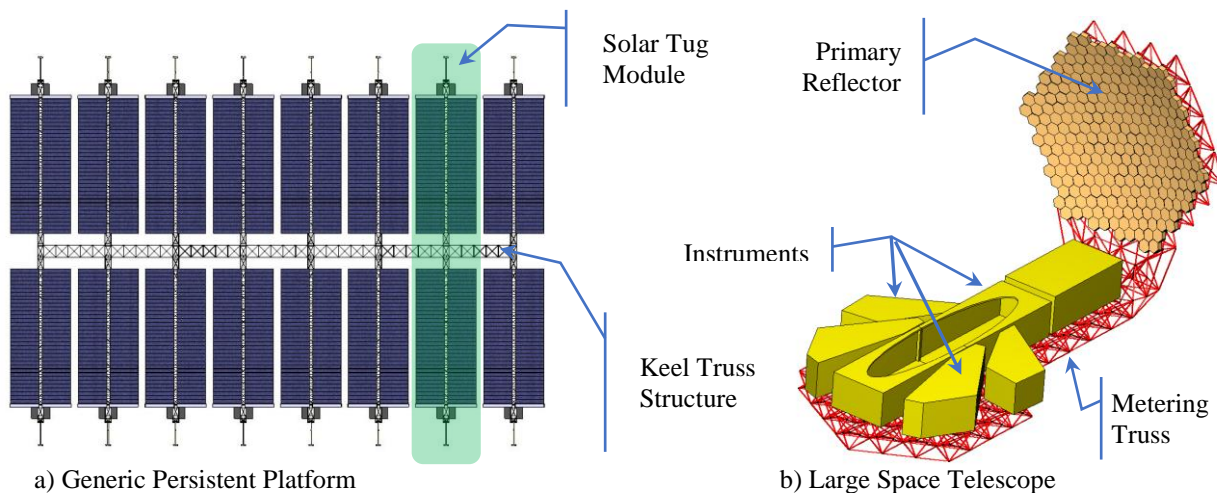
Fig. 1. Target missions for modular assembly.

This paper will introduce the TriTruss concept and describe how it can serve as the foundation for many different mission applications, in particular, a 20-meter diameter large space telescope and a beam-type platform that can host a variety of payloads and instruments. The geometry of the TriTruss will be described and the various truss design variables (such as truss depth, member diameter, material modulus, etc.) and each of their impacts on the truss performance will be illustrated. The TriTruss can be mapped to a variety of structural forms, such as beams, two-dimensional platforms and filled curved apertures (for antennas and telescopes) and examples will be illustrated. The TriTruss lends itself to a large variety of packaging schemes. The paper describes concepts associated with packaging and deployment, as well as the means for robotically deploying TriTruss modules and locking them into their final configuration. TriTruss module-to-TriTruss module robotic assembly operations will also be described. Appendix A contains equations that have been developed to structurally size TriTruss modules so that the assembled persistent platform achieves a specified global structural performance. A status of the TriTruss development will also be presented. This material will cover design and fabrication of TriTruss hardware for platform and telescope applications as well as structural testing of that hardware (the struts, connectors and platforms). Robotic assembly of TriTruss modules is also being performed, and the results of those tests will be summarized.

2. TriTruss: A New and Novel Structural Concept Enabling Modular Space Telescopes and Space Platforms

The erectable approach for in-space assembly of large space trusses, where the structure is assembled from individual struts and nodes, has been extensively studied and developed to a high degree of readiness as reviewed by Watson and Doggett[21,22]. While this approach directly supports construction of a wide range of structural forms, it necessitates that the utility systems, such as wiring harnesses and heat transfer systems, be routed and secured throughout the structure on-orbit. For large space telescopes, this approach also necessitates attaching the telescope reflector/support systems to the support truss on-orbit. In both cases, this severely limits the ability to validate subsystems prior to launch and extends the duration and complexity of the on-orbit operations. Some notional concepts have been developed to modularize the telescope and its architecture [13] by using deployable support trusses with integrated reflector segments (see Fig. 2), but most of these concepts suffer from mass inefficiency because there are redundant structural members along all of the intersecting boundaries.
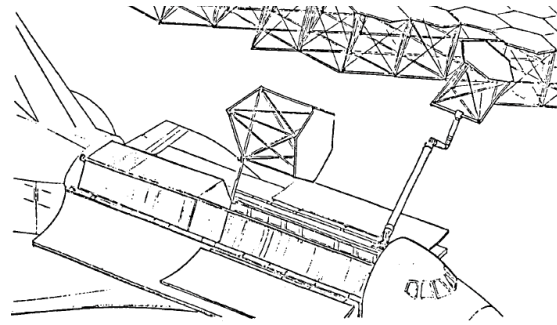

Fig. 2. Modular telescope concept with redundant structure at all interfaces.

In addition, these large space trusses have extensively embodied the geometry of the tetrahedral truss [23] as the primary reflector support system for a telescope, such as the trusses depicted in Fig. 2. For purposes of preliminary design, a fundamental frequency (associated with a required stiffness) is typically specified for the truss, and a truss sizing procedure is used to calculate the truss design parameters and mass. For these concept studies and preliminary design, large trusses can be accurately modelled as a sandwich plate, where the top and bottom surface strut members serve as the face sheets in the sandwich, providing axial and bending stiffness, and the core struts serve as the sandwich core, providing shear stiffness between the top and bottom faces. An efficient way to increase the truss stiffness (and thus meet a frequency constraint) is to increase its depth by lengthening the core struts (in relation to the face strut lengths). Generally, the same frequency constraint that is applied to the truss is also applied to the individual struts. Thus, a key limitation of a tetrahedral truss is that increasing its depth, increases all strut lengths, where as in the TriTruss module, only the core struts are affected.

In contrast to the historical approach described previously, recent work has concentrated on a new modular structural approach for architecting large space trusses. In Reference 20, a topological discussion is presented for two truss modules (one of which is the TriTruss) that are capable of being assembled into a beam, a platform, or a three-dimensional truss without duplicative members at the module interfaces. This topology is advantageous because it enables the design of predictable load paths with minimal structural mass and volume. Desired attributes of the new modular truss structure approach include: 1) assembly of truss modules using modular interfaces (not construction using individual truss members); 2) no duplication (redundant members) at the truss module interfaces; 3) ability to pre-integrate and test/validate systems (such as utilities, reflectors, etc.) on the ground before launch; 4) multiple possible locations for integrating systems on or within the truss module; 5) ability to increase truss depth (and

thus performance) efficiently; and 6) ability to stage truss module packaging according to the needs of embedded subsystems (packaged, partially packaged, not packaged). The TriTruss module has been conceived and is being developed to meet these six attributes.

The TriTruss module geometry (with integrated telescope reflector panels) is shown in Fig. 3a) for seven assembled modules and 3b) for a single module. Each module is a two layered system consisting of top and bottom members in the outer layers or faces, a central triangle in between (nominally halfway) the two outer faces, and core struts connecting the faces to the central triangle. The modular structural system is designed to behave similarly to a sandwich panel, with axially stiff top and bottom layers connected by core structural members that provide shear stiffness through the thickness (Fig. 3b). The top and bottom layers become isogrid structures, a very efficient structural form, with the primary load paths aligned with the center of these layers. The overall structural performance in an assemblage can be improved further if necessary by adding a small number of close-out structural members around the perimeter, installed in the top and bottom surfaces as shown in Fig. 3a or by adding additional TriTruss modules to provide this same structural closeout.

Now the TriTruss features which address the six attributes previously stated will be discussed. 1) Assembly of truss modules using modular interfaces to connect at the corners, as depicted in Fig. 3c – 3e (as opposed to previous construction where individual truss members were installed [15,21,22]). Here an example connector, a multi-nut, is shown. In this design, the multi-nut has three pre-integrated threaded holes to connect three modules at a node location. Multi-nuts are pre-attached to a module using a captive bolt (Fig. 3e), which is used to preload the interface between modules. This connection strategy is reversible, compact, and

a) Reflector Segmented with Hexagonal Panels

b) Stable TriTruss Module

c) Multi-Nut at Corner of TriTruss Module

d) Multi-Nut Connecting 2 Modules

e) Cross Section of Multi-Nut Connecting 3 Modules
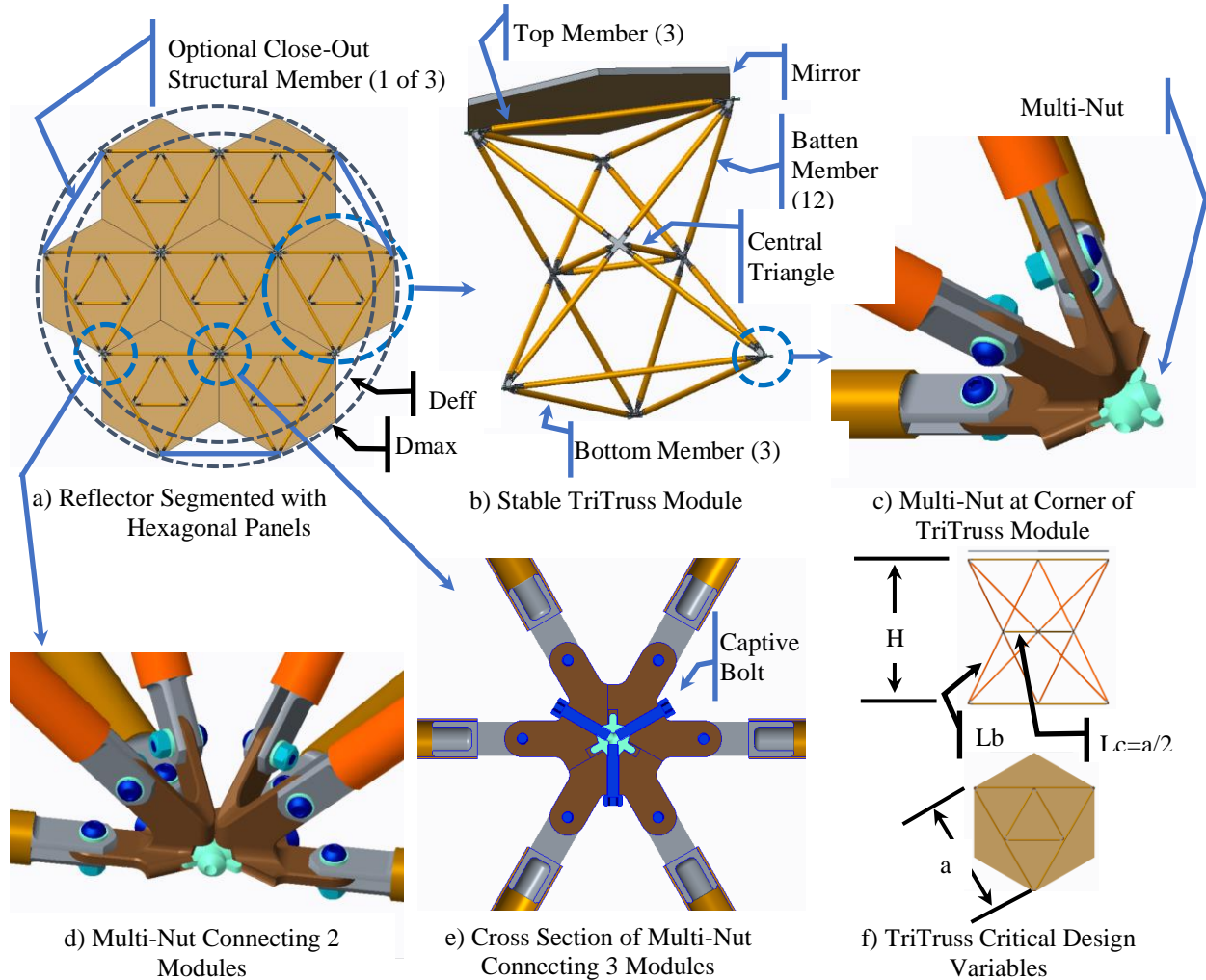
f) TriTruss Critical Design Variables

Fig. 3. TriTruss module geometry, definition, and metallic multi-nut connector.

lightweight. The connection strategy does not place any constraints on the order in which modules are removed, with each module maintaining a multi-nut in the top and bottom layers. Although it is most convenient to maintain multi-nuts at the same relative location in the top and bottom layers, this is not required.

2) No duplication (redundant members) at the truss module interfaces: The assembly of seven integrated TriTruss/mirror modules depicted in Fig. 3-a shows that the modules are connected at the corners, not along edges, so there is no redundant structure/struts in the assembly.

3) Ability to pre-integrate and test/validate systems (such as utilities, reflectors, etc.) on the ground before launch: Fig. 3b illustrates the ability to integrate a reflector panel with an individual TriTruss module, enabling a filled aperture to be achieved as shown in Fig. 3a. This is advantageous because it enables the panel and reflector assembly to be tested on the ground as an integrated unit, with the reflector positioning system fully integrated. This is one advantage of the modular approach; subsystems can be integrated and tested on the ground prior to launch, significantly reducing the programmatic cost and risk.

4) Multiple possible locations for integrating systems on or within the truss module: The TriTruss of Fig. 3 has numerous internal volume locations available for installing modular components, where "components" are sub-systems within a module that support module operations. Fig. 4 shows examples of volumes available for integrating components either as inscribed cylinders above or below the central triangle (Fig. 4a), or around the upper perimeter (Fig. 4b). When the TriTruss

modules are aggregated, the resulting system has numerous options for integrating components (Fig. 4c). Fig. 4c shows that entire equilateral triangle volumes are available between the TriTruss modules for additional component installation, either pre-integrated to the modules or installed after the TriTruss modules have been assembled. This space between modules is a result of the TriTruss geometry having the central triangle with a smaller diameter than the face triangles.

5) Ability to increase truss depth (and thus performance) efficiently: In Fig. 3f, the basic TriTruss module is defined as having 6 surface (both top and bottom) struts, a central triangle of 3 struts, and 12 batten struts with length dependent on the value of truss depth "H" chosen. Because its performance mimics that of a sandwich structure, increasing the H/a ratio will rapidly (increases as the square of the depth as discussed in the appendix) increase the structural stiffness. The central triangle effectively halves the core strut lengths (compared to the tetrahedral truss), leading to lighter mass struts that meet the strut frequency requirement.

6) Ability to stage truss module packaging according to the needs of embedded subsystems. The module may be launched in the configuration depicted in Fig. 3b, or may be packaged as depicted in Fig. 5a. Deployment from the packaged configuration to the operational configuration occurs as depicted in Fig. 5b, and is accomplished by telescopically retracting the central triangle. In addition, it is straightforward to package half of the TriTruss depth, either the portion below the central triangle (Fig. 5c) or the portion above the central triangle (Fig. 5d) by telescoping the appropriate struts.
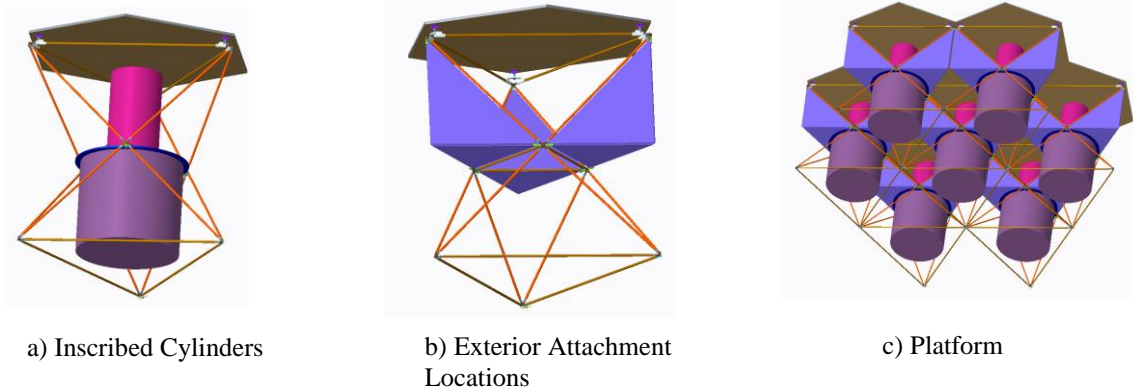

| a) Inscribed Cylinders | b) Exterior Attachment Locations | c) Platform |

Fig. 4. Representative volumes available for packaging components.

a)   Packaged TriTruss
(Fully Collapsed)

b) Deployment Sequence from a)

c) Partially Packaged TriTruss
below Central Triangle

d) Partially Packaged TriTruss
above Central Triangle
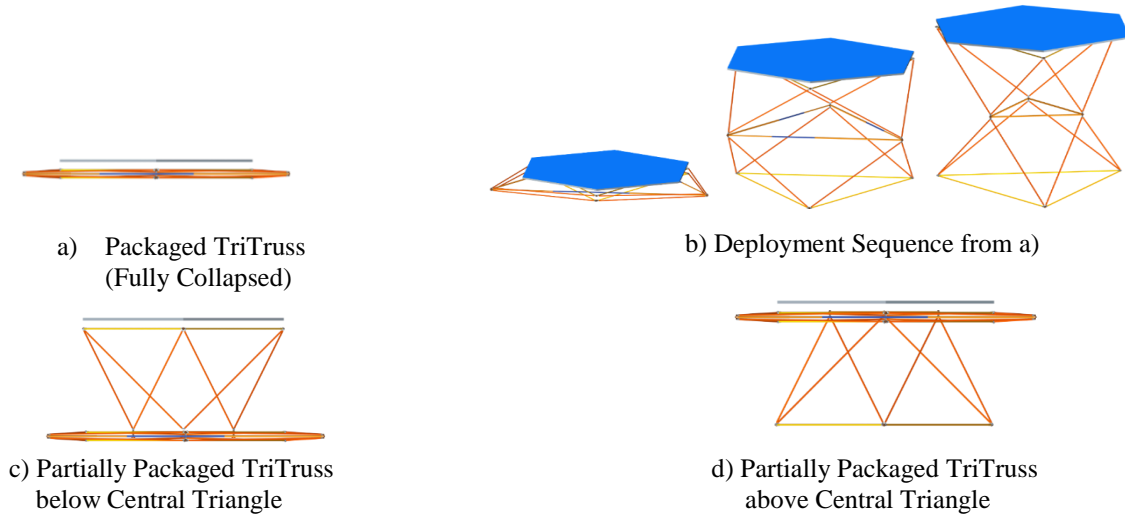
Fig. 5. TriTruss packaging options.

2.2 Telescope Structures Supported by TriTruss

a) Primary Mirror

c) TriTruss Supporting
7 Segment Rafts

b) Metering
Truss
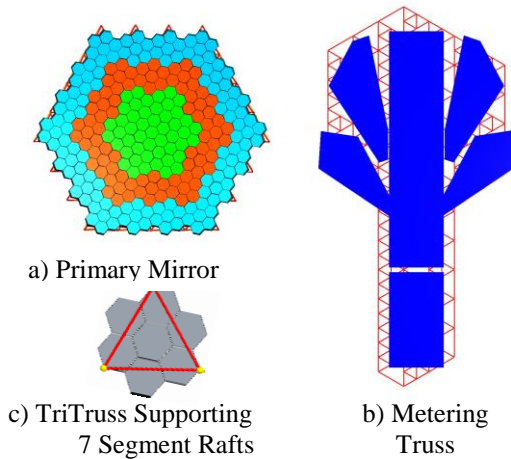
Fig. 6 TriTruss area structures.

The TriTruss architecture lends itself to area structures as well as beams. For the telescope depicted on the right of Fig. 1, the TriTruss is well suited to creating the primary reflector support, Fig. 6a, as well as the metering truss which supports the instruments which are shown in blue in Fig. 6b. Around the truss perimeters, shown in Figs. 3a and Fig. 6b, optional close-out struts may be necessary or additional TriTruss modules (without panels) can be used to provide the close-out.   The TriTruss architecture supports a variety of reflector grouping geometries. Fig. 6a depicts a primary reflector with 3 rings of mirror rafts (denoted by the different color zones) where each raft contains 7 hexagonal mirror segments (Fig. 6c) supported by a single TriTruss module.   Alternatively, Figs. 3a and 3b depicts a geometry where a single hexagonal panel is supported by each TriTruss module.

In a planar structure, such as the metering truss of Fig. 6b, all TriTruss modules can be the same, while in a curved architecture, such as the primary reflector of Fig. 6a, each TriTruss module is still the same, but the connection strategy has a unique geometry, though depending on the curvature, the differences between each connection may be small. However, in both cases, through careful design, the interfaces between modules and the tools used to assemble the modules can be uniform.   Appendix **AA**A provides a method for estimating the mass of the TriTruss system as a function of a variety of design variables.

3 Closing Comments.

Space operations are on the cusp of a revolutionary new operational paradigm that leverages modular systems and repeated robotic visits to "Persistent Assets" enabling asset maintenance, repair, and enhancement. A "Persistent Asset" (PA) is defined here as any near zero-gravity or planetary surface system that benefits from multiple visits.

The versatile TriTruss module, which can be used as the basis for planar or curved area structures, has been introduced. The module packages efficiently and, as will be described in detail in Appendix A can be easily customized to trade performance vs. mass. An important feature is that an assembly of modules acts like a large sandwich panel, having efficient isogrid face sheets separated by a lightweight core structure, producing a high performance structural system.

Detailed design trades are needed to explore the challenges and benefits associated with in-space assembly where much of the validation and verification occurs in-situ. Chief among the advantages is the long-

term ability to modify, upgrade, expand and enhance the system through multiple visits by servicing spacecraft.

Appendix A – Mass Model for a Free-Free Multi-Ring TriTruss Reflector

A.1 Introductory Remarks

In [24], a premise was put forth relative to the development of low-cost structures for new space systems. The premise was as follows:

"The first generation of space structural systems will almost certainly be produced in very limited numbers. This means that the costs of development cannot be spread over a large production quantity. Consequently, the largest cost of a space structural system will continue to be the cost of design, analysis, test, and all the systems engineering and tons of paperwork necessary to give adequate assurance that the system will perform as intended. The next largest cost will be launch and space erection. The smallest, by far, will be the manufacturing costs of materials, hardware, fabrication, assembly, and inspection. The engineer will therefore find only one practical way to design low-cost space structures: use approaches that reduce the cost of the design and development effort itself."

In [25], an associated and similar premise was put forth that *"Modeling is the Key to Engineering Design, and, Thus, Low-Cost Development."* The primary rational was *"The availability of validated models enables simulations that provide confidence that the system will behave as expected."* This reference goes on to postulate that *"This work is sequential in the sense that starting from an initial guess, the knowledge of the system grows, and models get more and more accurate and detailed as the work proceeds."*

The purpose of the preliminary design approach that is described in this appendix is to enable development of a model for support trusses that can be matured and built upon, eventually leading to a rational and reliable model to assist in the evolution of affordable structures for large precision apertures. Developing and maturing such a model will also enable rational comparisons with alternate reflector concepts in future system level studies.

The multi-ring TriTruss reflector model results in a closed-form solution for calculating the structural mass. The value of having a closed-form solution is that it enables rapid and rational parametric trade studies to be conducted allowing major drivers in precision reflector designs to be determined. For the example results presented in this study, it was necessary to make numerous assumptions that will require updating as data becomes available in the future.

A.2 Model Development Approach

For preliminary design purposes, the doubly curved parabolic truss reflector is treated as a flat sandwich circular plate as was done in [23, 24]. In this appendix, the truss is assumed to be made up of a number of rings, r, of TriTruss modules as shown in Fig. 3 and first presented in [20]. In the present analysis, the primary design constraint for the reflector is its free-free frequency. This is the same approach taken in [23], and all analysis assumptions and rationale proposed in that reference are used herein.

Specifically, the multi-ring array of hexagonal panels that form the reflector surface are supported by a corresponding array of TriTruss structures. This resulting reflector is treated as a simple circular sandwich plate, and the free-free frequency is determined using a conventional frequency equation for a circular plate. As discussed in [23], the resulting primary reflector depicted on the right of Fig. 1, is approximated as being circular as shown by the dashed lines in Fig. 3a. In this paper, the reflector reference diameter is taken as the diameter of a circle that has the same area as all of the hexagonal panels. The diameter is referred to as the effective diameter, D_{eff}. The reason for this reference choice is that the area associated with the effective diameter is that which would be available for electromagnetic reflection. Thus, for a given mass per unit area, m_p, the total panel mass is determined by multiplying by the area associated with D_{eff}. However, as discussed in [23], the diameter used for calculating the free-free frequency is the maximum diameter that circumscribes the reflector, D_{max}. The reason for using this larger diameter in the frequency equation as described in [23], is to heuristically account for transverse shearing and rotary inertia effects as determined from finite element analyses.

In [23], the structure presented was considered to be a tetrahedral truss. For a tetrahedral truss, the core members as well as the surface members are the same length. In the current paper, although all the truss surface members are all the same length, a, the depth of the truss, H, can vary, thus, changing the length of the core members. The resulting geometry and definitions are shown in Fig. 3f.

The mass of Nmodules of the TriTruss is given by equation 1. In this equation, a, is the length of the surface members that have a cross-sectional area, As. The global bending stiffness of the reflector truss structure is directly provided by the surface member axial stiffness, As. Since the core members do not contribute directly to the effective reflector plate bending stiffness, the core member area is taken as, β (As), where β is a factor to enable the core member cross-sectional area to be less than the surface member cross-sectional area. This is done since the core members represent a significant portion of the truss mass. The factor, α, is included in this analysis to allow a parametric study of effect of core member cross-sectional area on total TriTruss mass to be conducted. The factor, α, is the ratio of truss depth, H, to surface member length, a. Finally, ρ, is the density of

the members while, JF, is a factor included to account for truss joint mass.

The number of modules in equation 1 is given by the ratio of the reflector area given by Deff, divided by the area of a single reflector panel, Ap, as shown in equation 2. The area, Ap, of a single panel is given in equation 3 where the surface member length, a, is determined by a system level study that considers the individual module size due to launch vehicle payload fairing diameter as well as other parameters.

The effective bending stiffness, Dplate, of the resulting reflector structure as given by equation 4, is determined by assuming the top and bottom surface members provide an effective isotropic face sheet stiffness as discussed in [23], separated by a core of depth, H. The resulting mass per unit area of the complete reflector, m, is given by the sum of the reflector panel mass per unit area, mp, plus the mass per unit area of the TriTruss array as given by equation 5.

The lowest free-free frequency of the resulting reflector is given by equation 6, where the constant, Cf, is 3.345. As discussed previously, the frequency is calculated using the maximum plate diameter, Dmax. However, Dmax, is presented in terms of, Deff, in equation 7 to enable all example results to be presented in terms of the reference diameter, Deff. The ratio of diameters was obtained from Fig. A2 of [23].

A closed-form solution presented in equation 8 for the mass of the TriTruss support structure, MTriTruss, was obtained by simultaneously solving equations 1 through 7 in Mathematica. This equation can now be used to conduct parametric studies of the effects of changing any of the parameters in the equation. The solution for strut surface member cross-sectional area, As, is presented in equation 9. By knowing values for, MTriTruss, and for, As, all quantities in equations 1 through 7 can then be determined.
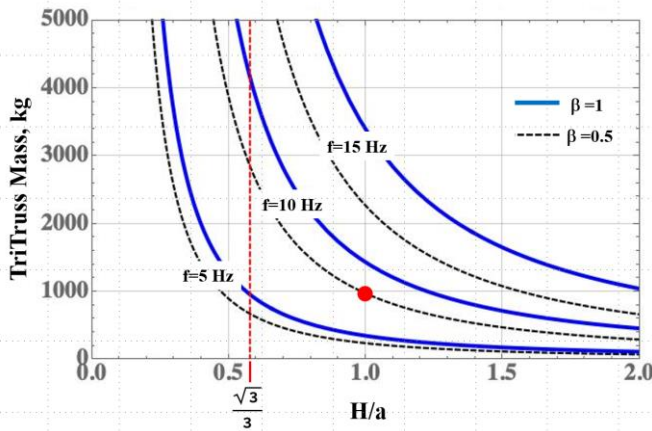

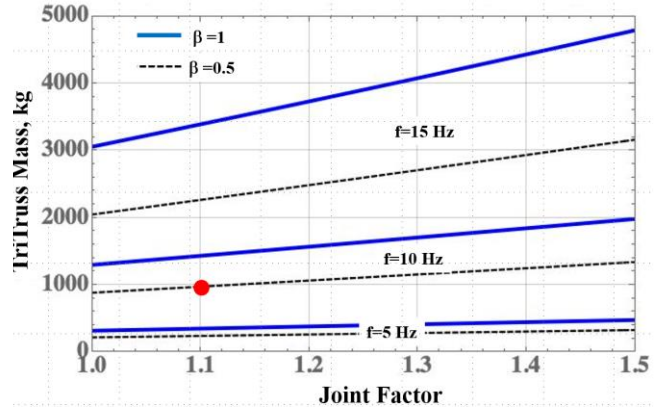
Fig. 7. TriTruss mass as a function of truss depth.

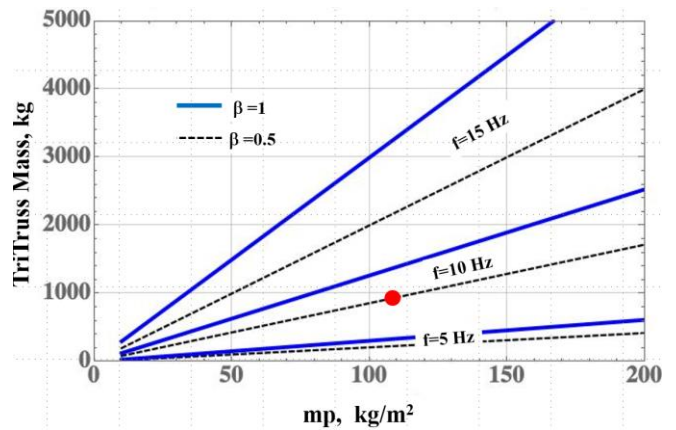Fig. 8. TriTruss mass as a function of joint factor, JF.

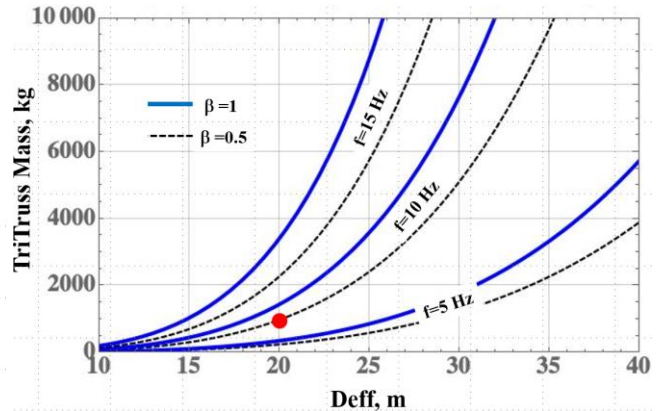Fig. 9. TriTruss mass as a function of panel mass per unit area, mp.

Fig. 10. TriTruss mass as a function of reflector effective diameter, Deff.

A.3 TriTruss Reflector Governing Equations

$$\text{MTriTruss} = \text{JF}\left(6a + 3\frac{a}{2}\beta + 6\beta\sqrt{a^2 + (\alpha a)^2}\right)(\text{As})(\rho)\text{Nmodules} \tag{1}$$

$$\text{NmodulesAp} = \frac{\pi\,\text{Deff}^2}{4} \tag{2}$$

$$Ap = \frac{\sqrt{3}}{2}a^2 \qquad (3)$$

$$DPlate = \frac{3}{8}\sqrt{3} \, As \, Ec \frac{(\alpha a)^2}{a} \qquad (4)$$

$$m = mp + \frac{MTriTruss}{\frac{\pi Deff^2}{4}} \qquad (5)$$

$$f = \frac{Cf}{Dmax^2}\sqrt{\frac{DPlate}{m}} \qquad (6)$$

$$Dmax = \frac{\sqrt{2\pi}}{3^{3/4}} Deff \qquad (7)$$

There are 7 equations for the 7 unknowns {MTriTruss, Ap, DPlate, As, Nmodules, m, Dmax}. Using Mathematica, the solution to the above 7 equations yields the following equations for the mass of the TriTruss system supporting the reflector and the area of the struts in the top or bottom plane of the TriTruss module.

MTriTruss =

$$\frac{4(\frac{\sqrt{2\pi}}{3^{3/4}})^4 Deff^6 f^2 JF(6a+3\frac{a}{2}\beta+6\beta\sqrt{a^2+(\alpha a)^2})mp\pi\rho}{9a^3 Cf^2 Ec\alpha^2 - 16(\frac{\sqrt{2\pi}}{3^{3/4}})^4 Deff^4 f^2 JF(6a+3\frac{a}{2}\beta+6\beta\sqrt{a^2+(\alpha a)^2})\rho} \qquad (8)$$

As =

$$\frac{8\sqrt{3}a^2(\frac{\sqrt{2\pi}}{3^{3/4}})^4 Deff^4 f^2 mp}{9a^3 Cf^2 Ec\alpha^2 - 16(\frac{\sqrt{2\pi}}{3^{3/4}})^4 Deff^4 f^2 JF(6a+3\frac{a}{2}\beta+6\beta\sqrt{a^2+(\alpha a)^2})\rho} \qquad (9)$$

A.4 Example Results

In the following sections five examples are presented of results from equations 8 and 9. In the first example, results of a point design are presented, while in the next four examples, equation 8 is used to establish parametric plots to demonstrate its applicability to the development of mass trend studies.

20 m Diameter Reflector Point Design Example. This point design example is for a 20-meter diameter reflector fabricated from composite struts for which the major design constraint is a global frequency of 10 Hz. The mass per unit area, 113.09 kg/m^2 for the hexagonal surface panels is assumed to include the mass of the truss-to-panel connectors and actuators as well as required utility lines. The input parameters are:

mp=113.09 kg/m^2; ρ=1626 kg/m^3; Ec=280 10^9 Pa, JF=1.1; Cf=3.345;Deff=20 m; r=3.; f=10; α=1; β=0.5 ; t=2.54 mm;

Calculate a, using

$$a = \sqrt{\frac{\frac{\pi Deff^2}{4}}{\frac{\sqrt{3}}{2}(3r^2 + 3r + 1)}}$$

Then the panel diameter is given by

$$PanelDiameter = \frac{2}{\sqrt{3}}a$$

From equations 8 and 9

As = 0.000426587 m^2(0.6612 in^2)

TriTruss Mass= 971.70279kg
Assuming a tubular strut, from

$$StrutDiameter = \frac{As}{\pi\, t}$$

the strut diameter can be found to be

Dstrut = 53.459 mm (2.1047 in)

In the current study, the only design constraint considered is the frequency of the free-free reflector system. For a given truss arrangement, this frequency is determined by the cross-sectional area of the struts, As, and the depth of the truss, H. For a resulting strut length and strut cross-sectional area, As, a secondary study must be conducted to determine the strut diameter and thickness. For this stiffness driven study, the necessary combination of strut diameter, and thickness must be determined from a number of factors, such as packaging, and practical thickness. In the above example, the thickness was assumed to be 2.54 mm (0.1 inches) which resulted in a strut diameter of 53.56 mm (2.1 inches). If these values are deemed adequate, the design is finished. If some other condition such as slenderness ratio or strut local frequency is not satisfactory, a different thickness can be selected until an acceptable design is found.

For this 20-meter diameter, 3-ring reflector, the length of the surface struts is 3.13 meters which is also the same dimension as the depth of the truss. The surface strut cross-sectional area required to provide a free-free frequency of 10 Hz is 426 mm^2 (0.66 in^2). It is further assumed that the surface struts are thin walled composite tubes with a thickness of 2.54 mm (0.1 inches). This assumed thickness results in a surface strut diameter of 53.56 mm (2.1 inches) and thus, a strut slenderness ratio, a/d, of approximately 60. Such a low slenderness ratio should be within acceptable engineering practice and result in a robust well-behaved truss structure under expected mechanical and thermal loadings.

However, in this example, in an attempt to reduce truss mass, an assumption was made that the cross-sectional area of the core members is ½ of the cross-sectional area of the surface members. Thus, engineering judgement must be exercised in establishing the core struts wall thickness and resulting diameter. If the same thickness is used as for the surface members, the slenderness ratio of the core struts will grow considerably. However, an alternative is to reduce the wall thickness to limit slenderness increase.

In the set of results shown in this Appendix, a red dot tracer is associated with the TriTruss mass for the assumed parameters of this example. In the next four charts, parametric plots are made varying parameters from the point design example. The red dot point design tracer is shown on each of the four subsequent charts to provide a quick reference back to the point design example case.

Parametric Plot of TriTruss Mass as a Function of Truss Depth. In Fig. 7, TriTruss mass is plotted from equation 8 for the same parameters as the point design case except that it is plotted as a function of truss depth for different values of frequency and β. The red dot tracer is shown as a reference to the truss mass of the point design case. As can be seen from the figure, both truss depth and required frequency are major drivers for the reflector truss mass. The vertical dashed line on the figure is for a truss that has the same depth as the tetrahedral truss of reference [26]. It can be seen from the tracer in the figure, that for the same required frequency, the mass of the point design example truss is about 1/3 that of one that is the depth of the tetrahedral truss (i.e. when $\frac{H}{a} = \frac{\sqrt{3}}{3}$). An additional observation from Fig. 7 is that a mass reduction on the order of 30% can be achieved by reducing the cross-sectional area of the core members to ½ of that of the surface members.

Parametric Plot of TriTruss Mass as a function of Joint Factor. In Fig. 8, TriTruss mass is plotted as a function of joint factor for different values of frequency and β. Again, the red tracer is shown as reference to the truss mass of the point design case. Although the joint factor is not as major a mass driver as truss depth or frequency, it is important to understand the trends to enable rational design tradeoffs.

Parametric Plot of TriTruss Mass as a Function of Panel Mass per Unit Area. In Fig. 9, TriTruss mass is plotted as a function of, mp, for different values of frequency and β. As can be seen from the figure, the truss mass increases linearly with respect to the panel mass per unit area, mp.

Parametric Plot of TriTruss Mass as a Function of Effective Reflector Diameter. In Fig. 10, TriTruss mass is plotted as a function of Deff for different values of frequency and β. For this case the truss mass grows approximately as the fourth power of the diameter. This rapid increase in truss mass with diameter is an indication of the increasing challenge that will occur for increasing reflector diameter. However, as is the case with essentially all very large structural systems, the approach for circumventing this inordinately large mass increase is to find means for operating at lower structural frequencies or make use of alternate approaches for stiffening the structure, such as adding layers to increase the structural depth.

Methods for dealing with low structural frequencies include using advanced metrology and control techniques and active control. An approach for increasing frequency is to incorporate guy cable stiffening into the architecture. Both approaches should be considered if larger reflector systems are pursued.

List of References
[1] Dorsey, J. T., Collins, T. J., Doggett, W. R., and Moe, R. V., "Framework for Defining and Assessing Benefits of a Modular Assembly Design Approach for Exploration Systems," Presented at the Space Technology and applications International Forum – STAIF 2006, Albuquerque, NM, 12 – 16 February 2006, AIP Conference Proceedings Volume 813, Editor Mohamed S. El-Genk, 2006 American Institute of Physics.
[2] Belvin, W. Keith, Dorsey, John T., and Watson, Judith J., "Technology Challenges and Opportunities for Very Large In-Space Structural Systems," Presented at the International Symposium on Solar Energy from Space, Toronto, Canada, Sept. 8 – 10, 2009.
[3] Dorsey, John T., Doggett, William R., Hafley, Robert A., Komendera, Erik, Correll, Nikolaus, and King, Bruce, "An Efficient and Versatile Means for Assembling and Manufacturing Systems in Space," Presented at the AIAA Space 2012 Conference and Exposition, 11 – 13 September 2012, Pasadena, CA, Available as AIAA-2012-5115.
[4] Dorsey, J., and Watson, J., "Space Assembly of Large Structural System Architectures (SALSSA)," Presented at the AIAA Space 2016 Conference, 13 – 16 September 2016, Long Beach, CA, Available as AIAA-2016-5481.
[5] Belvin, W. Keith, Doggett, Bill R., Watson, Judith J., Dorsey, John T., Warren, Jay, Jones, Thomas C., Komendera, Erik E., Mann, Troy O., and Bowman, Lynn, "In-Space Structural Assembly, "Applications and Technology," Presented at the AIAA SciTech Conference, 4-8 January 2016, San Diego, CA.
[6] Lymer, J., Doggett, W., Dorsey, J., Bowman, L, et. al., "Commercial Application of In-Space Assembly," Presented at the AIAA Space 2016 Conference, 13 – 16 September 2016, Long Beach, CA, Available as AIAA-2016-5236.
[7] Dorsey, J. T., Doggett, W. R., Moe, R. V., Ambrose, R. O., and Trevino, R. C., "Technology Validation for On-Orbit Assembled, Large Aperture Modular Space Telescopes," Presented at the Space Technology and Applications Forum (STAIF-2004), February 8 – 12, 2004, Albuquerque, New Mexico.
[8] Komendera, E., and Dorsey, J., "Initial Validation of Robotic Operations for In-Space Assembly of a Large Solar Electric Propulsion Transport Vehicle," (Not Presented due to Hurricane) AIAA Space and Astronautics Forum, 2017, 12 – 14 September 2017, Orlando, FL, Available as AIAA-2017-5248.
[9] Williams, L., Dorsey, J., and Foust, J., "GEO Communications Transponder Park: A New Concept for Direct Broadcast Services," Presented at the AIAA

Space 2003 Conference and Exhibition, 23 – 25 September 2003, Long Beach, California, Available as AIAA 2003-6316.

[10] Doggett, William R., Dorsey, John T., Collins, Timothy J., King, Bruce, and Mikulas, Martin M., "A Versatile Lifting Device for Lunar Surface Payload Handling, Inspection and Regolith Transport Operations," Presented at the Space Technology and Applications International Forum – STAIF 2008, Albuquerque, NM, 10 – 14 February 2008, AIP Conference Proceedings Volume 969, Editor Mohamed S. El-Genk, 2008 American Institute of Physics.

[11] Doggett, William R., King, Bruce D., Jones, Thomas C., Dorsey, John T., and Mikulas, Martin M., "Design and Field Test of a Mass Efficient Crane for Lunar Payload Handling and Inspection – The Lunar Surface Manipulation System," Presented at the AIAA Space 2008 Conference and Exposition, 9 – 11 September 2008, San Diego, California, Available as AIAA-2008-7635.

[12] Dorsey, John T., Jones, Thomas C., Doggett, William R., Brady, Jeffrey S., Berry, Felicia C., Ganoe, George G., Anderson, Eric J., King, Bruce D., and Mercer, C. David, "Recent Developments in the Design, Capabilities and Autonomous Operations of a Lightweight Surface Manipulation System and Test Bed," Presented at the AIAA Space 2011 Conference and Exposition, September 27 – 29, 2011, Long Beach, CA, Available as AIAA-2011-7266.

[13] Hedgepeth, John M., "Support Structures for Large Infrared Telescopes", NASA CR 3800, 1984.

[14] Vozoff, Max, and John Couluris. "SpaceX products-advancing the use of space." *AIAA SPACE 2008 Conference & Exposition*. 2008.

[15] Komendera, Erik, Reishus, Dustin, Dorsey, John T., Doggett, William R., and Correll, Nikolaus, "Precise Truss Assembly Using Commodity Parts and Low Precision Welding," In Proceedings of the IEEE Technologies for Practical Robot Applications, 2013.

[16] Komendera, Erik, Dorsey, John T., Doggett, William R., and Correll, Nikolaus, "Truss Assembly and Welding by Intelligent Precision Jigging Robots," In Proceedings of the IEEE Conference on Technologies for Practical Robot Applications, April 14 – 15, 2014, Boston, MA.

[17] Doggett, William R., Dorsey, John T., Jones, Thomas C., and King, Bruce D., "Development of a Tendon-Actuated Lightweight In-Space Manipulator (TALISMAN)," Presented at the 42nd Aerospace Mechanisms Symposium, NASA Goddard Space Flight Center, May 14 – 16, 2014.

[18] Doggett, William R., Dorsey, John T., Jones, Thomas C., Lodding, Kenneth N., Ganoe, George G, Mercer, Charles D, and King, Bruce D., "Improvements to the Tendon-Actuated Lightweight In-Space MANipulator (TALISMAN)," Presented at the AIAA Space 2015 Conference, August 31 – September 2, 2015, Pasadena, CA, Available as AIAA-2015-4682.

[19] Komendera, Erik E., Doggett, William R., Dorsey, John T., Debus, Thomas J., Holub, Kris, and Dougherty, Sean P., "Control System Design Implementation and Preliminary Demonstration for a Tendon-Actuated Lightweight In-Space MANipulator (TALISMAN)," Presented at the AIAA Space 2015 Conference, August 31 – September 2, 2015, Pasadena, CA, Available as AIAA-2015-4628.

[20] Doggett, William R., Teter, John E., Paddock, David A., Dorsey, John T., Jones, Thomas C., Komendera, Erik E., Bowman, Lynn M., Allen, Danette B., Neuhaus, Jason R., Taylor, Charles B., Mikulas, Martin M., Erandis, Ryan, and Mukhopadhyay, Rounak: Persistent Assets in Zero-G and on Planetary Surfaces: Enabled by Modular Technology and Robotic Operations. Presented at the AIAA Space 2018 Conference, Available as AIAA-2018-5305.

[21] Watson, Judith J., Timothy J. Collins, and Harold G. Bush. "A history of astronaut construction of large space structures at NASA Langley Research Center. *Proceedings, IEEE Aerospace Conference*. Vol. 7. IEEE, 2002.

[22] Doggett, William. "Robotic assembly of truss structures for space systems and future research plans. *Proceedings, IEEE Aerospace Conference*. Vol. 7. IEEE, 2002.

[23] Mikulas, Martin M., Jr., Collins, Timothy J. and Hedgepeth, John M., ``Preliminary Design Approach for Large High Precision Segmented Reflectors," NASA TM-102605, February 1990.

[24] Hedgepeth, John M., Mikulas, Martin M., Jr. and MacNeal, Richard H., ``Practical Design of Low-Cost Large Space Structures," Aeronautics and Astronautics, October 1978, pp. 30-34.

[25] Dobre, Tanase G. and Marcano, Jose G. Sanchez, "Chemical Engineering: Modeling, Simulation and Similitude", WILEY-VCH Verlag GmbH & Co. KGaA, Weinheim, ISBN: 978-3-527-30607-7, 2007.

[26] Mikulas, Martin M., Jr., Bush, Harold G. and Card, Michael F., ``Structural Stiffness, Strength and Dynamic Characteristics of Large Tetrahedral Space Truss Structures, NASA TM X-74001, March 1979.